Marine Pollution Bulletin 132 (2018) 33–43

Contents lists available at ScienceDirect

Marine Pollution Bulletin

journal homepage: www.elsevier.com/locate/marpolbul

Sequential webcam monitoring and modeling of marine debris abundance☆

Shin'ichiro Kako[a,*], Atsuhiko Isobe[b], Tomoya Kataoka[c], Kei Yufu[b], Shuto Sugizono[d], Charlie Plybon[e], Thomas A. Murphy[f]

[a] Graduate School of Science and Engineering, Department of Ocean Civil Engineering, Kagoshima University, Kagoshima, Japan
[b] Research Institute for Applied Mechanics, Kyushu University, Fukuoka, Japan
[c] Tokyo University of Science, Noda, Japan
[d] Faculty of Engineering, Department of Ocean Civil Engineering, Kagoshima University, Kagoshima, Japan
[e] Surfrider Foundation Oregon region, Oregon, USA
[f] Department of Fisheries and Wildlife, Oregon State University, Oregon, USA

ARTICLE INFO

Keywords:
Webcam monitoring
Japanese tsunami debris
Coastal upwelling/downwelling
Wind setup
Surf zone model

ABSTRACT

The amount of marine debris washed ashore on a beach in Newport, Oregon, USA was observed automatically and sequentially using a webcam system. To investigate potential causes of the temporal variability of marine debris abundance, its time series was compared with those of satellite-derived wind speeds and sea surface height off the Oregon coast. Shoreward flow induced by downwelling-favorable southerly winds increases marine debris washed ashore on the beach in winter. We also found that local sea-level rise caused by westerly winds, especially at spring tide, moved the high-tide line toward the land, so that marine debris littered on the beach was likely to re-drift into the ocean. Seasonal and sub-monthly fluctuations of debris abundance were well reproduced using a simple numerical model driven by satellite-derived wind data, with significant correlation at 95% confidence level.

1. Introduction

Marine debris from various sources and activities such as agriculture, fisheries, tourism, and industry—as well as illegal dumping and accidental losses from vessels—has pervaded marine ecosystems in the global ocean (e.g., Jambeck et al., 2015). Most marine debris is carried by both ocean surface currents and winds from domestic and overseas sources over long distances (hence long periods), and is then washed ashore on beaches (Gall and Thompson, 2015). Many studies (e.g., Gregory and Ryan, 1997; Derraik, 2002; Nakashima et al., 2012) have indicated that plastics account for ~70% of all marine debris washed ashore on beaches.

The large amount of debris drifting in the ocean constitutes a grave threat to marine life and ecosystems through ingestion and entanglement (Gall and Thompson, 2015), as well as through transport of hydrophobic persistent organic pollutants that adsorb onto plastic marine debris from seawater (Mato et al., 2001). Marine debris washed ashore on beaches also has impacts on coastal intertidal and/or supralittoral environments through invasive species attached to debris surfaces (Barnes, 2002), and carries a potential risk of harmful substances such as toxic metals leaching from the debris (Derraik, 2002; Nakashima et al., 2012). In addition to the aforementioned environmental risks, it has been recognized that marine debris diminishes the tourism value of beaches because of an aesthetically offensive form of pollution (Kako et al., 2010a, 2010b, 2011a, and Nakashima et al., 2011).

Despite the above concerns with marine debris, it remains difficult to hindcast and/or forecast the abundance of such debris washed ashore on beaches to determine the most effective frequencies of beach survey and/or beach cleanup activities. Marine debris abundance on a beach is a function of three fundamental and interrelated components, i.e., the concentration of debris in nearby waters, deposition on the beach, and re-drifting from the beach. Thus, the beach can be both a sink and a source of marine debris, regardless of season. Recent advances in atmosphere/ocean general circulation models and reanalysis products have provided reliable modeled winds and ocean currents, which are capable of supporting particle-tracking numerical models (e.g., Isobe et al., 2009; Kako et al., 2010a, 2011a, 2014) that reproduce marine debris behavior in the oceans. Nonetheless, unresolved in these models are complex debris motions in surf zones forced by tides, coastal currents, waves and winds, and local topography. In addition, it is difficult to reproduce exchange processes (i.e., washing ashore and re-drifting) of marine debris between surf zones and beaches. Therefore, particle-

☆ This is one of the papers from the special issue of Marine Pollution Bulletin on "The effect of marine debris caused by the Great Tsunami of 2011." The special issue was supported by funding provided by the Ministry of the Environment of Japan (MOE) through the North Pacific Marine Science Organization (PICES).

* Corresponding author at: Department of Ocean Civil Engineering, Kagoshima University, 1-21-40 Korimoto, Kagoshima 890-0065, Japan.
E-mail address: kako@oce.kagoshima-u.ac.jp (S. Kako).

https://doi.org/10.1016/j.marpolbul.2018.04.075
Received 26 January 2017; Received in revised form 19 April 2018; Accepted 30 April 2018
Available online 30 May 2018

tracking models are unlikely to reliably reproduce marine debris on beaches unless the above nearshore processes are incorporated appropriately.

A straightforward way to reproduce the nearshore processes is to establish a surf zone model that can be incorporated into particle-tracking models, which is the objective of the present study. The model is specialized to reproduce washing-ashore and re-drifting processes associated with atmospheric and oceanic conditions such as winds, waves and ocean currents, as well as the offshore abundance of marine debris. Therefore, it is necessary to identify the fundamental and interrelated components mentioned above (hereafter, "critical factors") to reliably determine variability in marine debris abundance on beaches.

A number of methods have been developed to quantify debris abundance on shorelines (e.g., Kako et al., 2010b, 2012; Kataoka et al., 2012; Veenstra and Churnside, 2012). Aerial photography using small aircraft is useful to search and document long stretches of inaccessible coastlines to estimate the relative abundance of debris (Veenstra and Churnside, 2012). However, aerial photography provides only snapshots of beaches, although it can cover extensive remote areas quickly and relatively easily. To establish the surf-zone model, we used marine-debris monitoring with a webcam, which takes beach photographs once per hour. As with aerial photography, conventional beach surveys (e.g., once per month) are insufficient for capturing the temporal variability of debris abundance resulting from atmospheric and oceanic processes with typical timescales shorter than fortnightly spring/neap tidal cycles and/or sub-weekly passages of extratropical cyclones (Kako et al., 2011a). Our previous studies (Kako et al., 2010b; Kako et al., 2012, and Kataoka et al., 2012) demonstrated that the area covered by marine debris and its temporal variation can be computed from webcam photographs via the image processing methods proposed in those studies. The sequential (once every 60–90 min) webcam monitoring system established in these previous studies are capable of capturing the variation of marine debris abundance on time scales shorter than a month. Thus, webcam monitoring is likely more suitable for resolving temporal variations of marine debris abundance than in-situ visual and manual beach surveys.

The webcam monitoring was conducted on a beach along the western coast of the United Sates to monitor marine debris related to the Great Tohoku Earthquake, which triggered a massive tsunami on March 11, 2011. According to estimates by the Ministry of the Environment, Government of Japan (https://www.env.go.jp/en/focus/docs/files/20120901-57.pdf), about 5 million tons of Japanese tsunami marine debris (JTMD) flowed away from Japan into the North Pacific. Part of this JTMD (estimated at 1.5 million tons) remained afloat and is still drifting in the North Pacific. Thus, there is a concern for this debris reaching the North American and Hawaiian coasts. In particular, attention is given to coastal Japanese species carried by the JTMD. In fact, the National Oceanic and Atmospheric Administration reported that "in the case of a dock, it carried a biofouling community that included over 90 marine species that were not native to the West Coast of North America" (https://marinedebris.noaa.gov/sites/default/files/Japan_Tsunami_Marine_Debris_Report.pdf). Thus, these species have the potential to damage the indigenous marine ecosystem along beaches of North America and the Pacific islands (Murray et al., 2015).

Nevertheless, there have been no published studies investigating temporal variations of marine debris abundance on beaches along the western U.S. and Canadian coasts over a period longer than 1 year (including seasonality) and with monitoring intervals shorter than a week. Consequently, there is no way of knowing the critical factors governing temporal variations of debris abundance on these beaches. In the present study, using a dataset of marine-debris abundance monitored by the webcam system, we establish a simple but reliable surf zone model based on the critical factors to hindcast the temporal variation of debris abundance on the western U.S. and Canadian coasts.

2. Material and methods

2.1. Webcam

We installed a webcam on a beach in Newport, Oregon, USA (Fig. 1), because it directly faces the North Pacific and is free from complex topography, and because it has easy access for installing/maintaining the webcam. In addition, community residents told us that substantial marine debris washes ashore on the beach. The webcam was set up to sequentially and automatically take photographs of a part of the beach on which marine debris was littered, including driftwood and anthropogenic debris (possibly including JTMD). Beach photographs were taken every 60 min during daytime (10 times from 9:00 AM to 6:00 PM Pacific Standard Time in the USA) from April 3, 2015 to March 31, 2016 (this webcam observation ended in April 2017). The area, approximately 60 m × 70 m in the alongshore and offshore directions, respectively, was photographed within the entire panorama by the webcam with a fixed angle. An accurate angle was not required because we counted debris number visually. In addition, the camera angle was not required, even if we computed an accurate area covered by marine debris via image processing such as projection transformation. This is because reference positions are given on each photograph for georeferencing (Magome et al., 2007; Kako et al., 2012). These photographs were transmitted to our web server via the Internet. Actual JTMD was difficult to identify from the photographs, unless the debris source was suggested by Japanese characters printed on the debris surface and those characters were sufficiently large to be identified on the photographs.

It was found that a substantial amount of marine debris (mostly driftwood and lumber) was washed ashore on the beach over a 1-year period from the start of monitoring (Fig. 2a shows an example of photographs taken by the webcam). Nonetheless, anthropogenic debris such as plastic was difficult to identify on the photographs. It was also difficult to distinguish lumber from natural driftwood. However, nearshore processes determine the motion of drifting objects, regardless of whether they are artificial. Thus, marine debris monitored by the webcam was analyzed without discrimination between natural and anthropogenic debris, to elucidate critical factors governing the temporal variation of debris abundance on the beach.

The abundance of marine debris was evaluated by counting their number (N) on the beach photographs by visual observation. The camera angle (hence, the entire beach area covered by the webcam) was fixed over the survey period, so number per unit area was obtained by $N/(60\,\text{m} \times 70\,\text{m})$. Likewise, $N/100\,\text{m}$ (frequently used in marine debris surveys; e.g., Ryan et al., 2009) is computed as $N \times 100/70$. It is indeed reasonable to compute the difference in brightness and colors of pixels to extract marine debris from the background beach (Kako et al., 2010b; Kako et al., 2012; Kataoka et al., 2012; Nakashima et al., 2012). However, these methods were not available for the present study, because there was little difference in both brightness and color between the sandy beach and driftwood/lumber (Fig. 2a).

First, an observer selected a single photograph from all 10 photographs taken on each day. The photograph was selected to identify marine debris to the extent possible during daytime. Thus, photographs at ebb tide (i.e., the broadest beach area) were likely to be selected, whereas those during foggy and/or rainy periods were removed. Thereafter, the observer identified the marine debris, irrespective of its size, as shown by red circles in Fig. 2b. This is because the motion (trajectory) of a floating object is determined only by the ratio between projected areas above and below the sea surface in conjunction with the speeds of ambient ocean currents and winds (rather than by object size). If small objects were difficult to distinguish from shadows of surface irregularity on the beach, the remaining nine photographs at various times (different incident angles of sunlight) were used for the

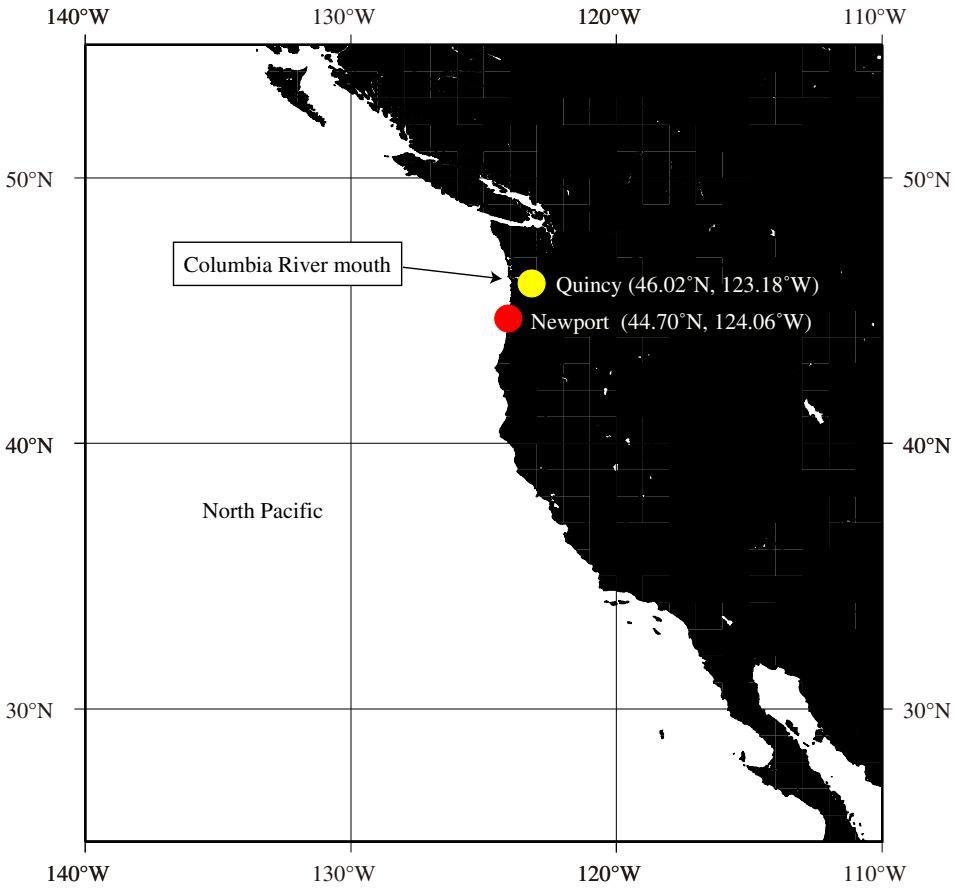

Fig. 1. Locations of webcam monitoring site in Newport, Quincy (river discharge observatory), and Columbia River mouth.

identification. To reduce human error in counting the marine debris, visual observations were made twice by different observers, double-checking omissions and/or duplications of the debris.

2.2. Satellite-derived sea surface wind speed, dynamic height, and sea surface temperature

The temporal variation of marine debris abundance on the beach was compared with that of satellite-derived meteorological and oceanographic data, to investigate potential causes(s) of that variation. Marine debris is carried by winds (leeway drift) (Richardson, 1997) and ocean currents, so we used a global gridded wind vector dataset (0.25° longitude × 0.25° latitude resolution) constructed via an optimum interpolation method (Kako et al., 2011b) applied to the Level 2.0 Advanced Scatterometer (ASCAT) wind product (i.e., instantaneous values) (Verspeek et al., 2009; KNMI, 2010). This product was downloaded from the Physical Oceanography Distributed Active Archive Center at the Jet Propulsion Laboratory (https://podaac.jpl.nasa.gov). The gridded dataset used herein is freely available from the website http://mepl1.riam.kyushu-u.ac.jp/~kako/ASCAT. Sea surface height (SSH) above the geoid (i.e., absolute dynamic topography) provided an effective indicator of ocean currents by geostrophy and of ocean temperature by thermal expansion. Thus, we used a multi-satellite SSH dataset produced by Ssalto/Duacs (Segment Sol multi-missions dALTimetrie, d'orbitographie et de localisation précise/Data unification and Altimeter combination system) and distributed by AVISO (Archiving, Validation, and Interpretation of Satellite Oceanographic Data, with support from Le Centre national d'études spatiales; http://www.aviso.altimetry.fr/duacs/). This dataset is available from January 1993 at spatial resolution 0.25° longitude × 0.25° latitude and daily temporal resolution.

To depict maps of sea surface temperature (SST), we used the microwave optimum interpolation sea surface temperature (OI SST) dataset, which is produced by Remote Sensing Systems sponsored by the National Oceanographic Partnership Program and NASA Earth Science Physical Oceanography Program (data available at http://www.remss.com). The critical factors governing marine debris abundance around the webcam monitoring site were investigated by correlation analysis of the abundance and atmospheric/oceanic properties such as wind.

3. Results

3.1. Marine-debris abundance monitored by webcam

The time series of daily marine debris abundance derived from the webcam shows fluctuations on various timescales (Fig. 3). The raw data (black curve in that figure) shows irregular increases in debris abundance with a timescale shorter than a month. This highly variable time series demonstrates that monthly marine debris surveys are insufficient to resolve marine debris variation because of contamination by aliasing errors, which is pseudo long-term fluctuation revealed by coarsely subsampled time series with short-term fluctuations; see classical textbooks on random data analysis such as Bendat and Piersol (1971). Since the raw data had occasional missing values owing to camera mechanical problems and adverse weather conditions, it is difficult to focus on variation time scales shorter than weekly (i.e., sub-weekly variation). These missing values were linearly interpolated, and thereafter the time series was smoothed by a 7-day running mean to remove sub-weekly fluctuations. Thus, we focused only on intermediate processes longer than weekly but shorter than seasonal timescales.

A remarkable seasonality was revealed in the smoothed time series (red curve in Fig. 3), in which the abundance of marine debris gradually

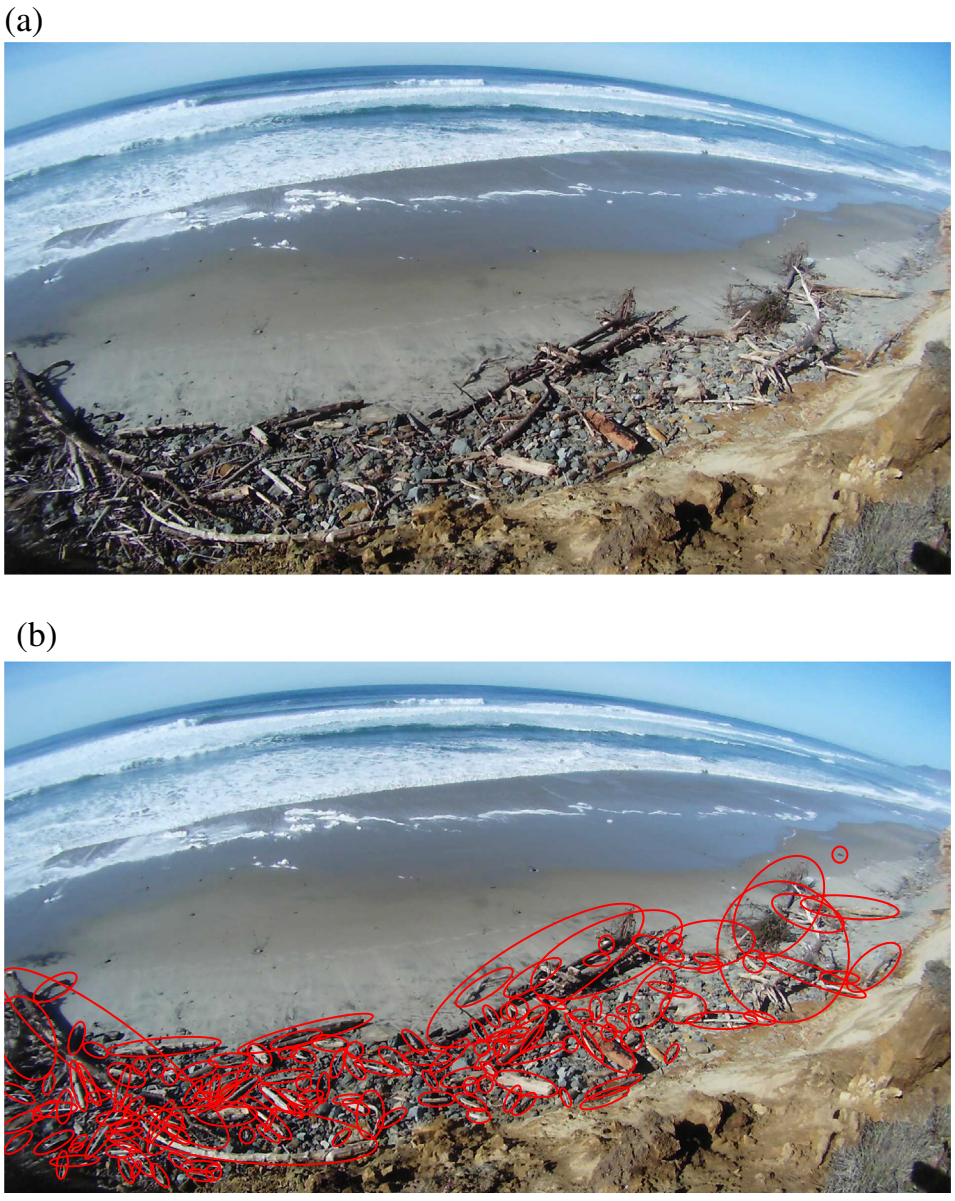

Fig. 2. Photographs of Newport beach on February 25, 2016, taken by webcam.
(a) Original photograph and (b) marine debris (surrounded by red circles) identified on the photograph by visual observation. (For interpretation of the references to color in this figure legend, the reader is referred to the web version of this article.)

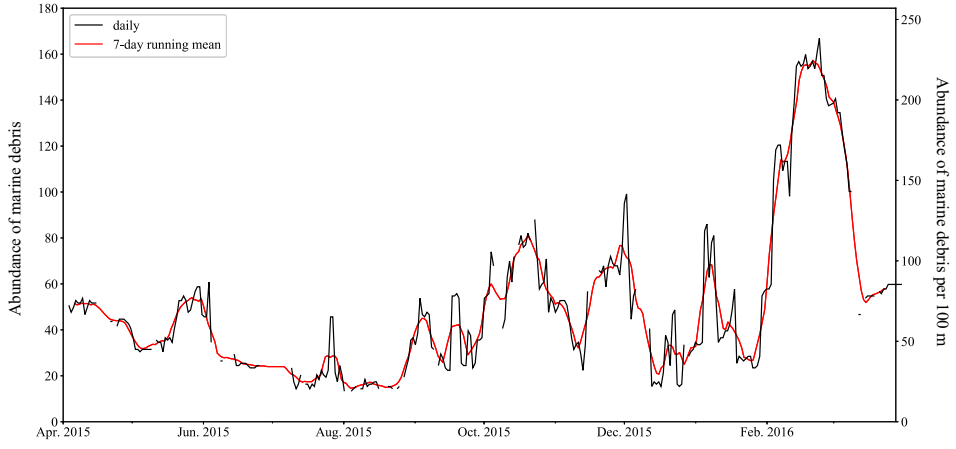

Fig. 3. Time series of number of marine debris, derived from webcam observation. Black curve indicates number counted on a photograph selected each day. Red curve is from smoothing using a 7-day running mean. Left (right) ordinate is used for numbers on entire photograph (each 100-m alongshore length). (For interpretation of the references to color in this figure legend, the reader is referred to the web version of this article.)

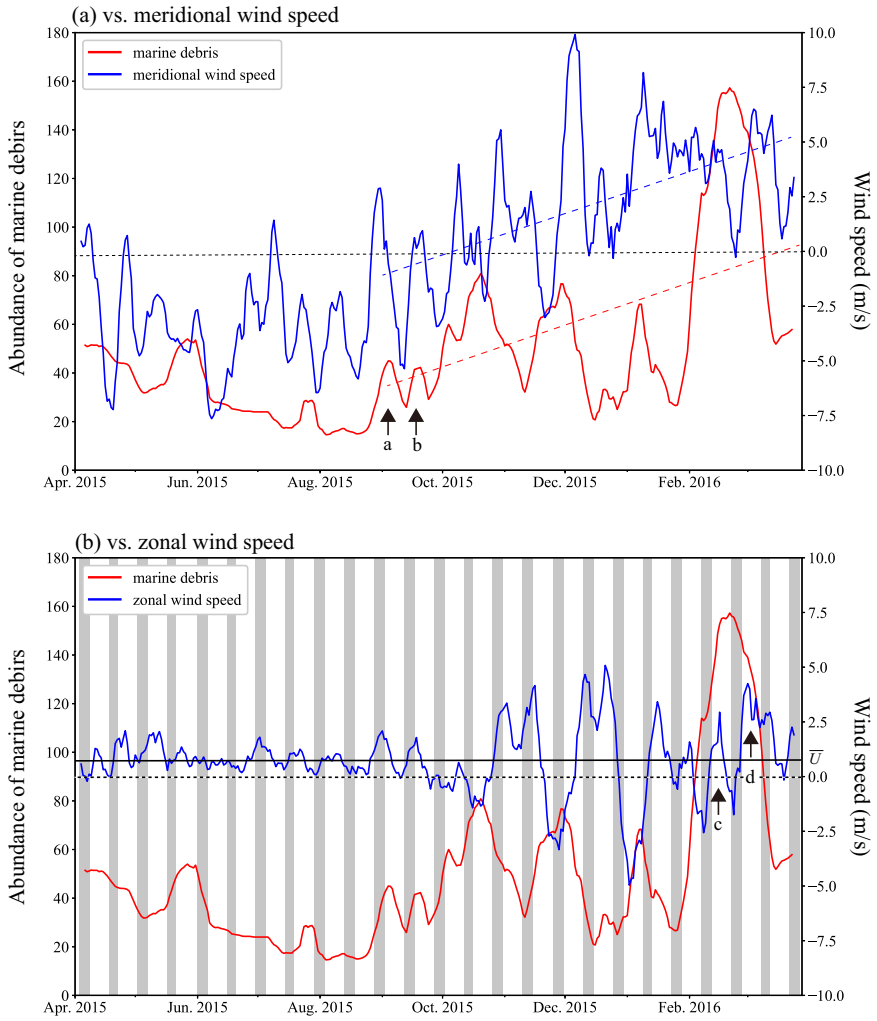

Fig. 4. Comparison of marine debris abundance with wind speed components. Debris abundance (red curves) is depicted with (a) meridional wind speed and (b) zonal wind speed, respectively. Positive values in (a) indicate southerly (northward) wind, and those in (b) westerly (eastward) wind. Red (blue) dotted line in (a) indicates linear trend of marine debris abundance (meridional wind speed) between September and March. Gray bars in panel (b) indicate period of spring tides. (For interpretation of the references to color in this figure legend, the reader is referred to the web version of this article.)

increased from the end of summer (September) through winter to the beginning of March. In addition to this seasonal increase, fluctuations on a timescale of one month or less (hereafter, sub-monthly) are clearly evident. The decrease of abundance was caused by natural re-drifting of individual debris items from the beach into the ocean. Cleanup was not conducted on the beach during the webcam observation period.

3.2. Comparison with satellite-derived wind speed, SSH and SST

Winds (leeway drifts) and wind-induced currents have a major role in the motion of floating objects in the ocean. Thus, it is worthwhile to compare the temporal variation of marine debris abundance on the beach with that of sea surface winds observed by ASCAT at the grid point (44.625°N, 124.125°W) nearest Newport Beach (Fig. 1). Since leeway drift is debris motion in the downwind direction as mentioned above, we can evaluate the effect of that drift on beach debris abundance using wind speed components, without computing leeway drift itself. Daily data smoothed by the 7-day running mean are used for comparison hereafter. Positive values in Fig. 4a indicate southerly (northward) wind, and those in Fig. 4b indicate westerly (eastward) wind. Meridional (north–south) and zonal (west–east) components are identical to alongshore and on–offshore components, respectively (Fig. 1).

The meridional wind component was responsible for seasonal (summer to winter) increase of debris abundance. In fact, the seasonal increase was revealed when southerly winds prevailed because of the development of the Aleutian low over the North Pacific; compare the two linear trends between September and March in Fig. 4a (dashed line). Unlike the aforementioned seasonal increase, it is difficult to find positive correlation between local maxima of the abundance (i.e., sub-monthly fluctuations) and the meridional wind component, except for the maxima shown by arrows a and b in Fig. 4a. In fact, the correlation coefficient (0.16) between marine debris abundance and meridional wind speed was not significant at the 95% confidence level over the same period, because the time series of meridional wind speed was likely to include fluctuations shorter than that of marine debris abundance (Fig. 4a). It should be noted that the local maxima of debris abundance, shown by arrow a in Fig. 4a, was likely to be delayed relative to that of the meridional wind speed component. This owes to the time needed for drifting debris to be moved by wind and ocean currents, so that it may be subsequently washed ashore, onto the beach, via nearshore processes.

The sub-monthly fluctuations of debris abundance appeared to be inversely related to the zonal wind component, especially from mid-October to the end of the study period. There was a significant negative correlation (coefficient = −0.58) at the 95% confidence level between marine debris abundance and zonal wind speed from mid-October to the end of January (Fig. 4b), when zonal wind fluctuations were

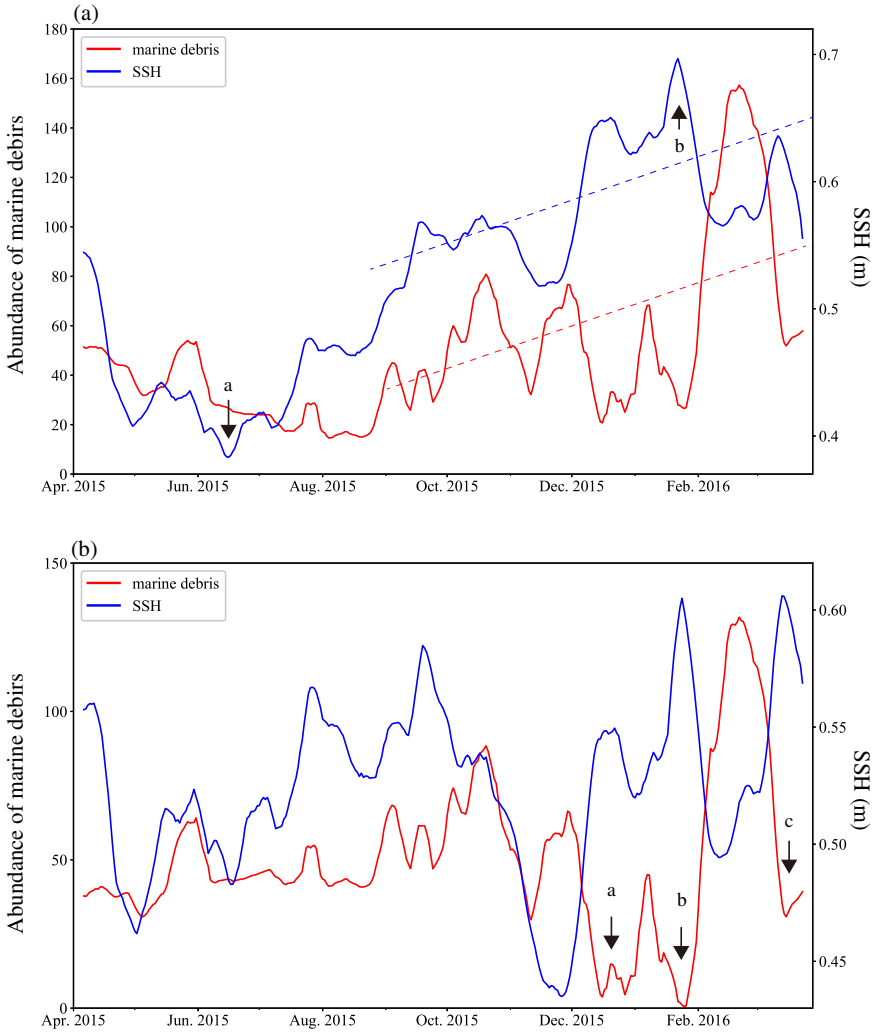

Fig. 5. Comparison of marine debris abundance with (a) SSH smoothed by 7-day running mean, and (b) SSH after removal of seasonal variation from panel (a). Red (blue) dotted line in (a) indicates linear trend of marine debris (SSH) between September and March. (For interpretation of the references to color in this figure legend, the reader is referred to the web version of this article.)

activated by the frequent passage of extratropical cyclones in the North Pacific (not shown). Marine debris decreased when westerly (shoreward) winds prevailed in winter. The removal of debris was likely to occur more rapidly than debris buildup on the beach; therefore, the debris abundance fluctuated almost in phase with the zonal wind speed component in winter. The debris abundance seemed to vary in a non-intuitive manner, because shoreward winds were likely to carry floating objects onto the beach because of wind-induced leeway drift. In fact, negative correlation was not always the case as shown by the two arrows c and d in Fig. 4b; debris abundance continued to increase despite a sub-monthly enhancement of shoreward winds.

In addition to the time series of debris abundance and wind speed, time series of SSH produced by AVISO also shows a seasonal increase from September to the beginning of March, as shown by the linear trends in Fig. 5a (dashed line). Moreover, when the seasonal variation was removed by fitting a sinusoidal curve minimizing least squares (Fig. 5b), temporal variations of SSH and debris abundance varied in an opposite sense between the first and last half of the study period. In the time series through the beginning of October, the sub-monthly fluctuations of debris abundance correlated positively with SSH (correlation coefficient = 0.52, significant at the 95% confidence level). In contrast, the abundance in winter rapidly decreased when the SSH time series exhibited local maxima at sub-monthly timescale (arrows a, b, and c indicating this rapid decrease in Fig. 5b).

The SST field off the Oregon coast drastically changed between the periods before and after the seasonal increase of SSH (hence the marine debris abundance). The SST map (Fig. 6a) reveals a southward extension of a low-SST band along the entire western coast of North America, when SSH had the smallest value during the study period (arrow a in Fig. 5a). Thereafter, when SSH maximized in January 2016 (arrow b in Fig. 5a), the low-SST band was replaced by a relatively high SST band along the entire western coast (Fig. 6b). These relationships between winds, SSH, SST and marine debris abundance are more closely examined in the next section.

4. Critical factors governing marine-debris abundance

4.1. Comparison with coastal upwelling/downwelling

It has been well known that coastal upwelling occurs along the western U.S. and Canadian coasts, especially during summer (http://oceanservice.noaa.gov/education/kits/currents/03coastal4.html) (Duxbury et al., 2002). Thus, the seasonal increase of marine debris during southerly winds along these coasts suggests a dependence of debris abundance on the occurrence of “coastal downwelling” and its associated shoreward Ekman transport (Ekman, 1905). When the southerly (downwelling-favorable) winds prevail, it is likely that the shoreward Ekman transport carries marine debris toward the coast and

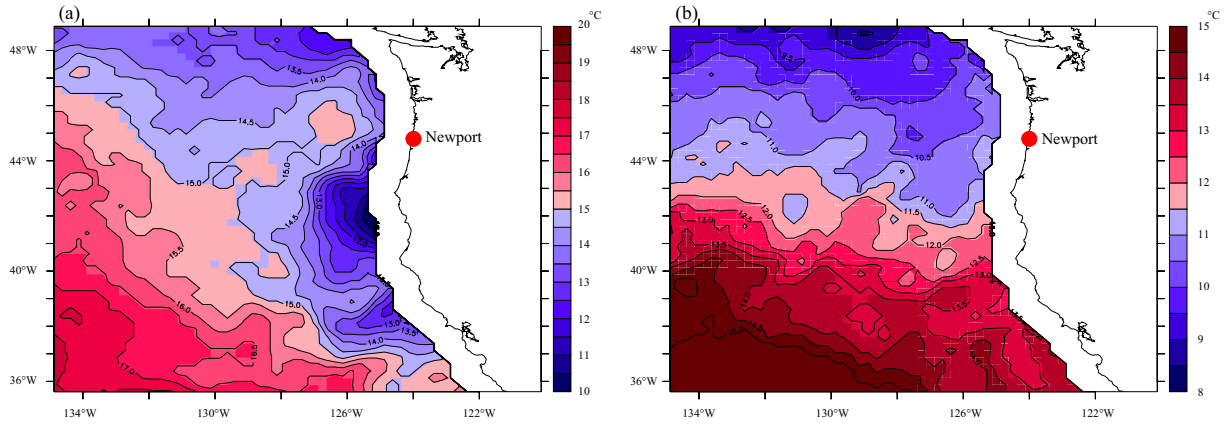

Fig. 6. Horizontal distribution of sea surface temperature on (a) June 15, 2015 and (b) January 19, 2016 when coastal upwelling and downwelling occurred along western coast of United States and Canada. Color bar ranges are different between (a) and (b).

that the debris littered on the beach subsequently increases (Fig. 7a). The beach litter decreased when drifting marine debris were prevented from approaching the coast because of offshore-ward Ekman transport induced by northerly (upwelling-favorable) winds (Fig. 7b). These findings are consistent with seasonal variation of meridional winds and marine debris abundance (Fig. 4a). Besides the seasonal increase, the probability of marine debris washing ashore on the beach was likely to increase whenever downwelling-favoring southerly winds (shoreward Ekman transport) prevailed transiently (e.g., arrows a and b in Fig. 4a). Nonetheless, as mentioned above, the meridional winds had a minor role in determining the sub-monthly fluctuations of debris abundance. This is because the positive correlation is negligibly small and the sub-monthly signals of debris abundance, especially in the first half of the period (April to beginning of October), were weaker than projected from the strong oscillation of the meridional winds (Fig. 4a).

In addition to the satellite wind data, the contribution of coastal downwelling to the seasonal increase of debris abundance was confirmed by investigating SSH. This is because SSH increases over the course of coastal downwelling events because of the pileup of seawater around the coasts and thermal expansion via the accumulation of warm surface water in the upper layer (Figs. 6b and 7a). In particular, SSH reveals downwelling events by upward displacement of SSH and vice versa (Fig. 7). This is consistent with the seasonal increase of debris abundance under the downwelling-favorable (southerly) wind (Figs. 4a and 5a). Ekman transport induced by northerly wind moves surface waters away from the coast and induces coastal upwelling (Fig. 7b). As a result, surface water is replaced by deep cool water that wells up from below (Figs. 6a and 7b), and marine debris abundance on the beach decreases (Fig. 7b; Fig. 5a for summer).

In contrast with the seasonal trend mentioned above, sub-monthly increases of marine debris abundance were not always concurrent with the upward displacement of SSH (Fig. 5b). In the first half, there was positive correlation between SSH and marine debris abundance on a sub-monthly timescale, while SSH was negatively correlated with that abundance on the same timescale in the second half (Fig. 5b; Section 3.2). This paper does not delve into the mechanism as to why the debris

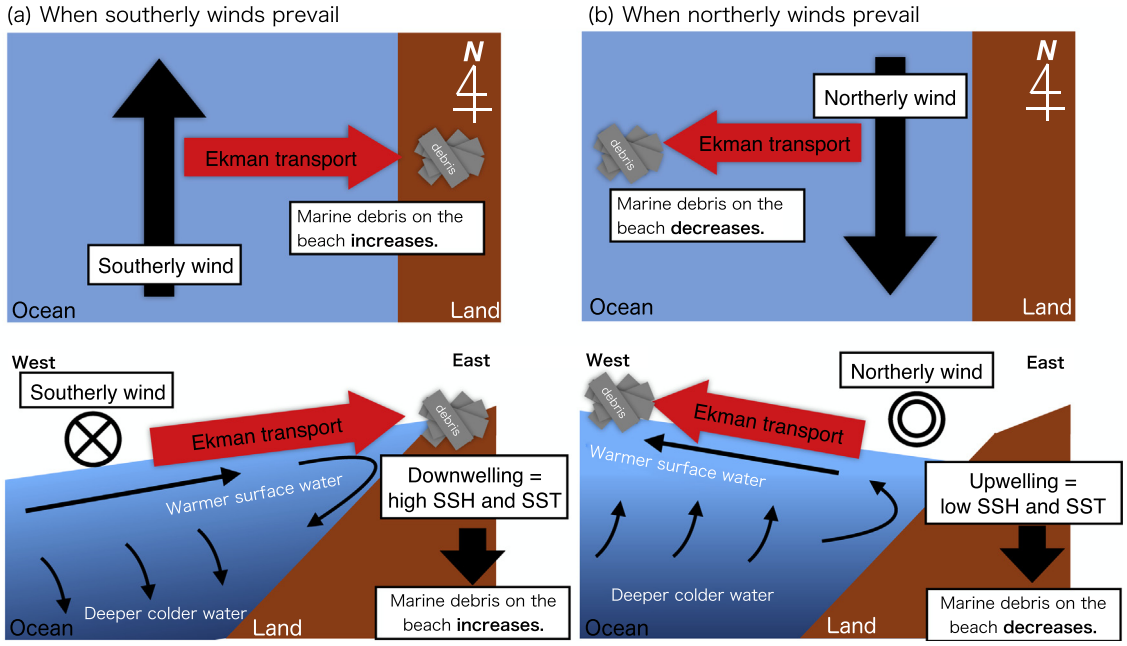

Fig. 7. Schematic diagram of relationship between wind direction and abundance of marine debris on the beach when winds blow along west coasts in Northern Hemisphere: (a) When southerly winds prevail, they induce shoreward Ekman transport. Coastal waters therefore pile up and coastal downwelling occurs, and marine debris abundance increases on the beach. (b) When northerly winds prevail, they induce offshore-ward Ekman transport. Surface warm water along the coast is replaced by deep cool water through coastal upwelling, and marine debris abundance on the beach decreases.

abundance transiently increased in accord with the sub-monthly upward SSH displacement in the first half of the study period. This is because sub-monthly fluctuations in the first half were much weaker than those in the last half. Explanation regarding sub-monthly fluctuations of winds, SSH, and debris abundance in the last half are addressed in the next subsection.

4.2. Wind setup by westerly (shoreward) winds at spring tide

A decrease of marine debris abundance occurred when westerly winds prevailed in the last half of the study period (Fig. 4b), regardless of the intensification of northerly winds (hence coastal upwelling; Fig. 4a). It is also interesting that in the last half, the debris abundance minimized when westerly winds prevailed around spring tides (gray bars in Fig. 4b). Simultaneous occurrence of westerly winds and spring tides was not a prerequisite for minimal debris abundance, as shown by January 2016. It is likely that individually, the westerly winds and spring tides are favorable for decreasing the abundance of marine debris, although the combination of the events worked effectively to reduce marine debris abundance.

It is reasonable to consider the occurrence of the wind setup (local sea-level rise caused by winds) and resultant re-drifting of debris littered on the beach on sub-monthly timescales, because debris abundance decreased during westerly (shoreward) winds (Fig. 4b), spring tides (Fig. 4b; particularly flood tide), and upward displacement of SSH (Fig. 5b) in winter. A photograph of the beach on December 11, 2015, when westerly winds prevailed at the first spring tide, reveals that the high-tide line moved landward over the entire beach (middle of Fig. 8). Thus, it is likely that seawater across the entire beach "swept" the debris from the beach (December 13; lower portion of Fig. 8). A schematic diagram of this process is illustrated in Fig. 9. It is believed that the beach tends to be excavated in winter, so re-drifting occurs more straightforwardly than in summer because the debris is unlikely to be buried deeply in the sand. In addition, the abundance of marine debris in summer was much less than that in winter (Fig. 3), so it is likely that the re-drifting was not clearly evident in the summer photographs.

4.3. Validation of two critical factors using a simplified model experiment

Two critical factors govern both seasonal and sub-monthly variations of the abundance of marine debris littered on the beach. One is coastal upwelling/downwelling and the other is the wind setup enhanced by shoreward (westerly) wind, especially at spring tides. Considering these results, we constructed a straightforward model to validate whether these two factors (or their combination) determine the variation of marine debris abundance on the beach. The relationship between marine debris abundance on the beach (N) and wind speed components in the meridional (V) and zonal (U) directions at the grid cell nearest Newport were simply modeled as follows.

$$N(t + \Delta t) = N(t) + a \times R(t), \tag{1}$$

where $N(t + \Delta t)$ is the number of marine debris at time $t + \Delta t$ and Δt is the time increment of model iteration; one day was chosen for the present application. R is the number of marine debris adrift in the area near Newport beach (hereafter, "offshore abundance"), and a is a non-dimensional parameter representing the "switch" that allows marine debris to wash ashore, as follows.

$$\begin{cases} a = 1, & if\ V > 0 \\ a = 0, & if\ V < 0 \\ a = -\frac{N(t)}{R(t)}, & if\ U\ at\ the\ spring\ tides > \overline{U} \end{cases}, \tag{2}$$

where $\overline{U}$ represents the average zonal wind speed (westerly wind of 0.74 m/s; see solid line in Fig. 4b) over the entire period. The two criteria in Eq. (2) represent the dependence of marine-debris abundance on the occurrence of coastal upwelling/downwelling, so that the debris number on the beach increases only under southerly winds (downwelling-favorable; $V > 0$). The third criterion in Eq. (2) represents the removal of marine debris on the beach (i.e., $N(t + \Delta t) = 0$) after establishment of the wind setup under westerly winds at spring tides stronger than the average over the entire period (U at spring tide $> \overline{U}$). The third criterion has priority over the other two criteria; otherwise, the debris would not decrease during winter.

The choice of offshore abundance of marine debris ($R(t)$) is somewhat arbitrary in the present application, but is given in accord with the abundance of modeled particles at the grid cell nearest to the beach when we conducted separate particle-tracking models. For simplicity, however, two different cases of $R(t)$ were assumed. First, the spatial distribution of offshore abundance was assumed to be homogeneous, so $R(t)$ was set to a constant ($R(t) = 1$) irrespective of time (case 1). The variation of marine debris abundance derived from our model was normalized by its standard deviation after removing the average value, so our results do not depend on the choice of $R(t)$ value in this case. What we compared was not the absolute value of marine debris abundance but the fluctuating abundance normalized by its standard deviation. To be sure, this implicit assumption that marine debris concentrations in proximate ocean regions are essentially the same is in discussion to some degree. Therefore, the second assumption is that offshore abundance is proportional to discharge of the river near the beach (case 2). Although it may seem a slight leap, we used this assumption because much of the debris littered on Newport Beach consisted of driftwood (Fig. 2), which likely had terrestrial sources around Oregon (rivers, bays, and estuaries) rather than overseas. The daily-mean Columbia River discharge observed at Quincy, Oregon (46.02°N, 123.18°E; Fig. 1) available on the U.S. Geological Survey website (https://www2.usgs.gov/water/) was used for $R(t)$ values in case 2. River discharge normalized by the minimum value over 1 year was taken as offshore abundance in case 2. Thus, the increase of river discharge indicates the increase of the offshore abundance of marine debris, and vice versa.

Overall, the model including the two critical factors reasonably reproduced the temporal variation of marine debris abundance on the beach (Fig. 10). Correlation and determination coefficients between webcam observation and the two model runs are respectively 0.85 and 0.72 in case 1, and 0.82 and 0.67 in case 2, all significant at the 95% confidence level. In particular, the "calm" period through September (see bar A in Fig. 10), strong fluctuations from October through the end of January (bar B), and a prominent peak in February (bar C) were all well reproduced in the modeled time series. The statistically significant correlation and determination coefficients between observed and modeled debris abundance suggests that the temporal variation of debris abundance was well explained by a linear combination of two critical factors. It also suggests that in determining the temporal variation of debris abundance on this beach, oceanic and atmospheric conditions (i.e., the critical factors) are more important than the terrestrial signal related to river discharge, because both model runs could significantly reproduce the variation of marine debris abundance. It is worth emphasizing that the modeled abundance was set to zero in accord with the onset of westerly winds stronger than a threshold (solid line in Fig. 4b). Thus, modeled maxima always delay the observations. This is because the actual beach debris was likely to partially return to the ocean under the modest westerly winds (i.e., modest wind setup). This is a limitation of our linear model. The remaining difference between model and observation in Fig. 10 was likely partially from the variation of offshore debris abundance and nonlinearity, although a predictive (prognostic) model is required for these processes to be incorporated.

5. Conclusions

The objective of the present study was to uncover critical factors determining the temporal variation of debris abundance washed ashore on

Fig. 8. Photographs of the day before (December 9, 2015), during (December 11), and after (December 13) westerly winds prevailed at spring tide. The change of ground form just below the webcam resulted from a landslide caused by a storm on December 11.

the beach at Newport by sequential and automatic monitoring using a webcam system, and to establish a surf zone model reproducing the temporal variation of debris abundance. The webcam could monitor a large amount of marine debris (mostly driftwood and lumber) on the beach, although it is difficult to perform detailed classification of debris items because of limited photograph resolution. Debris number per 100-m of beach fluctuated from 30 to > 250 items (Fig. 3), which was compared with recent values provided by Ryan et al. (2009) (see their Fig. 2). Sub-monthly fluctuations in our study with magnitude of O(100) items/100-m were remarkable compared with Ryan et al. (2009). This is probably because beach surveys with sample frequency longer than one month (Table 1 in Ryan et al., 2009) are too coarse to monitor the temporal variation of marine debris abundance on beaches. Finding the appropriate sample frequency is a goal in webcam monitoring of specific beaches.

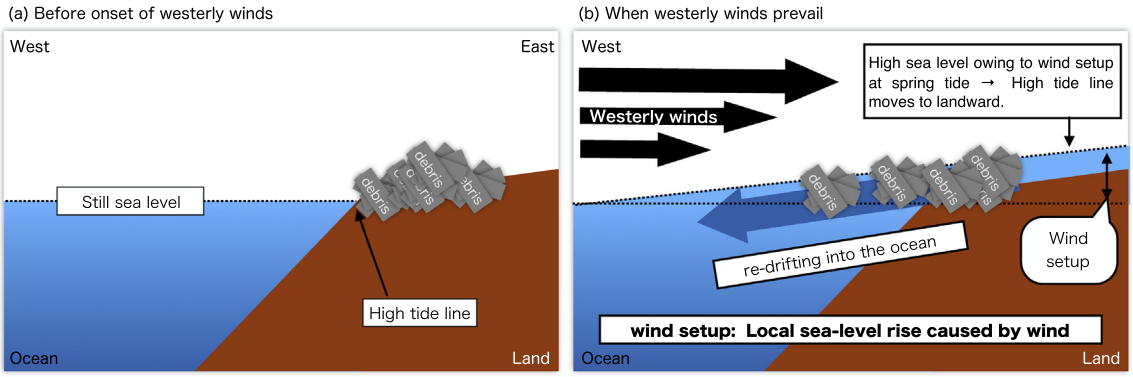

Fig. 9. Schematic diagram of re-drifting processes of marine debris when westerly winds prevailed at spring tide.

The strong temporal variation of marine debris abundance was compared with satellite-derived sea surface wind and SSH at the point nearest the beach. It was found that the temporal variation of debris abundance was governed by two critical factors, i.e., the occurrence of coastal upwelling/downwelling and wind setup amplified at spring tides. Offshore-ward Ekman transport (hence coastal upwelling) induced by northerly winds prevent offshore marine debris from approaching the beach, whereas shoreward Ekman transport (coastal downwelling) forced by southerly winds is key to the debris washing ashore (schematic diagrams of Fig. 7). In addition to the coastal upwelling/downwelling, the wind setup forced by shoreward winds at spring tides (and flood tides) causes re-drifting of the marine debris accumulated on the beach into the ocean (schematic diagrams of Fig. 9). These critical factors were highlighted by the simplified model, which reproduced the actual temporal variation of debris abundance with significant correlation.

It is anticipated that the model will be capable of reproducing marine debris abundance on various beaches along the western U.S. and Canadian coasts. Fig. 6 demonstrates that coastal upwelling/downwelling occurs along those coasts. Fig. 11 illustrates that there are westerly winds over the broad area offshore of these coasts in winter, and indicates that the wind setup at spring tides occurs simultaneously over the entire coast. These results indicate that the criteria of Eq. (2) using alongshore and across-shore components of sea surface winds are not unique to Newport Beach. In addition, coastal upwelling/downwelling occurs along various coasts directly facing the open ocean. Therefore, the present model should be capable of reproducing the variation of marine debris abundance on other beaches of the world, unless those beaches are behind an island or headland, or within a channel.

Particle-tracking numerical models have been widely used for reproducing marine debris adrift on the open ocean (Isobe et al., 2009; Kako et al., 2010a, 2011a, 2014). However, it remains a challenge as to whether particles approaching coasts are washed ashore, because nearshore processes are not well resolved in particle-tracking models conventionally used in marine debris studies. The present study identified a missing link between basin-scale ocean dynamics and beach observations by incorporating a surf-zone model established on the basis of sequential monitoring of marine debris on beaches. A large-scale model reproducing marine debris behavior in the open ocean can reproduce a more accurate R value in Eq. (1). Thus, a combination of the large-scale model and the surf-zone model established in the present study will reproduce more accurate temporal variation of beach debris abundance. In this combined model, the abundance of modeled particles at the grid cell nearest the beach in the large-scale model is capable of determining R values in Eq. (1). We have already established a combined model to hindcast JTMD abundance on the western U.S. and Canadian coasts; see our preliminary report in Isobe et al. (2017).

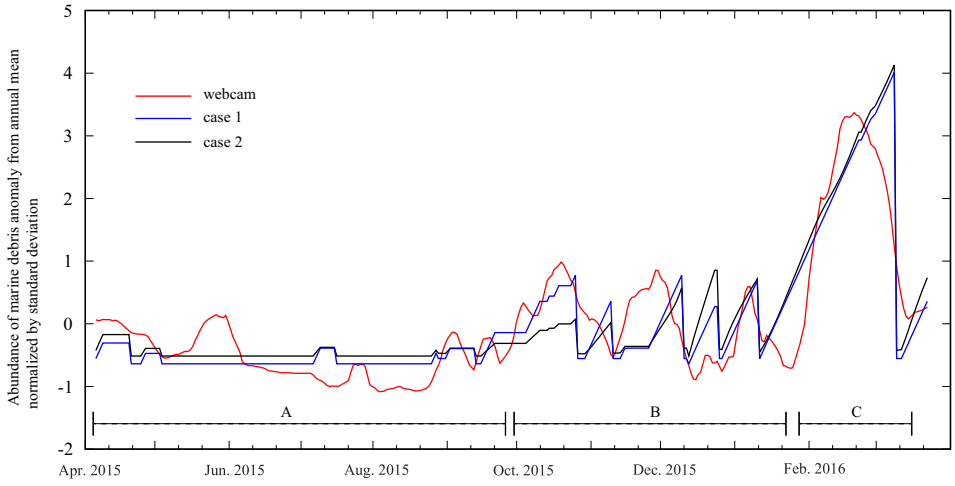

Fig. 10. Time series of abundance of webcam-observed (red curve) and modeled (black and blue curves) marine debris. In case 1, $R(t)$ was set to a constant ($R(t) = 1$) irrespective of time. In case 2, daily-mean Columbia River discharge observed at Quincy, Oregon was used for $R(t)$. Bar A indicates "calm" period through September, bar B strong fluctuations from October through end of January, and bar c a prominent peak in February. (For interpretation of the references to color in this figure legend, the reader is referred to the web version of this article.)

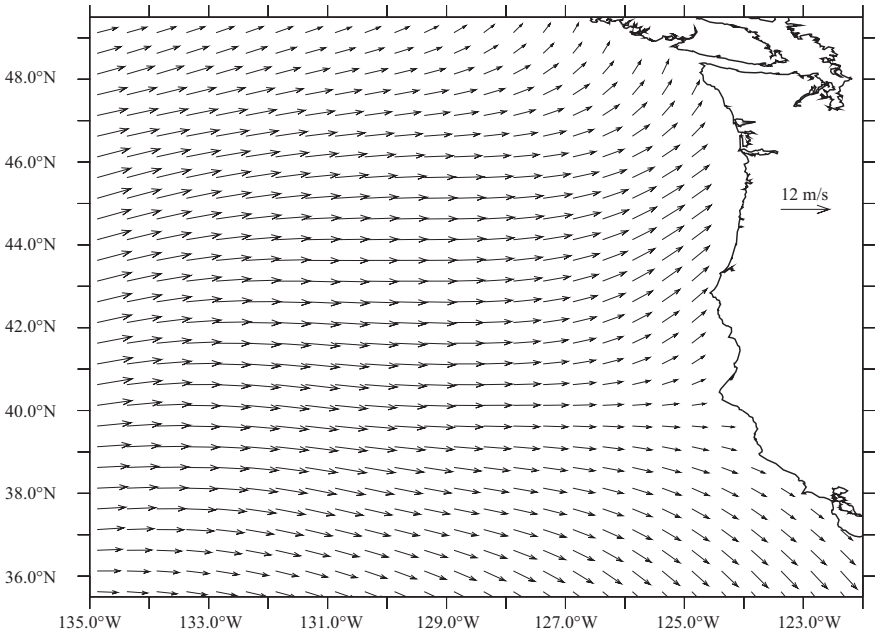

Fig. 11. Horizontal distribution of monthly wind field derived from ASCAT for December 2015.

Acknowledgments

This research was funded by the Ministry of the Environment of Japan through the North Pacific Marine Science Organization (PICES). We are grateful to the NASA EOSDIS Physical Oceanography Distributed Active Archive Center (PO.DAAC) at the Jet Propulsion Laboratory, Pasadena, California (https://podaac.jpl.nasa.gov), Archiving, Validation, and Interpretation of Satellite Oceanographic Data (AVISO) with support from Cnes (Le Centre national d'études spatiales; http://www.aviso.altimetry.fr/duacs/), Remote Sensing Systems (http://www.remss.com) sponsored by the National Oceanographic Partnership Program and NASA Earth Science Physical Oceanography Program, and the U.S. Geological Survey (https://www2.usgs.gov/water/) for providing satellite observations and river discharge data. We appreciate Dr. Nir Barnea for his help in installing the webcam in Newport, and a member of our technical staff, Mr. Masato Motoi, who patiently counted debris numbers on the photographs. We thank Steven Hunter, M.S., from Edanz Group (www.edanzediting.com/ac) for editing a draft of this manuscript. The two anonymous reviewers' comments and suggestions helped us improved our manuscript substantially.

References

Barnes, D.K.A., 2002. Biodiversity: invasions by marine life on plastic debris. Nature 808–809.
Bendat, J.S., Piersol, A.G., 1971. Random Data: Analysis and Measurement Procedures, 4th Edition. Wiley 640 pp.
Derraik, J.G.B., 2002. The pollution of the marine environmental by plastic debris: a review. Mar. Pollut. Bull. 44, 842–852.
Duxbury, N., et al., 2002. Fundamentals of Oceanography, 4th edition. McGraw Hill, New York 344 pp.
Ekman, V.W., 1905. On the influence of the earth's rotation on ocean currents. Arch. Math. Astron. Phys. 2 (1), 1–53.
Gall, S.C., Thompson, R.C., 2015. The impact of debris on marine life. Mar. Pollut. Bull. 92, 170–179.
Gregory, M.R., Ryan, P.G., 1997. Pelagic plastic and other seaborne persistent synthetic debris; a review of Southern Hemisphere perspectives. In: Coe, J.M., Rogers, D.D. (Eds.), Marine Debris – Sources, Impacts and Solutions. Springer-Verlag, New York, pp. 49–66.
Isobe, A., Kako, S., Chang, P.-H., Matsuno, T., 2009. Two-way particles tracking model for specifying sources of drifting objects: application to the East China Sea Shelf. J. Atmos. Ocean. Technol. 26, 1672–1682.
Isobe, A., Kako, S., Kataoka, T., Iwasaki, S., Plybon, C., Murphy, T.A., 2017. Webcam monitoring and modeling of Japanese tsunami marine debris washed ashore on the western coast of the North America. PICES Press 25 (1), 32–35.
Jambeck, R.J., Geyer, R., Wilcox, C., Sieger, R.T., Perryman, M., Andrady, A., Narayan, R., Law, K.L., 2015. Plastic waste inputs from land into the ocean. Science 347, 768–771.
Kako, S., Isobe, A., Seino, S., Kojima, A., 2010a. Inverse estimation of drifting-object outflows using actual observation data. J. Oceanogr. 66, 291–297.
Kako, S., Isobe, A., Magome, S., 2010b. Sequential monitoring of beach litter using webcams. Mar. Pollut. Bull. 60, 775–779.
Kako, S., Isobe, A., Magome, S., Hinta, H., Seino, S., Kojima, A., 2011a. Establishment of numerical beach litter hindcast/forecast models: an application to Goto Islands, Japan. Mar. Pollut. Bull. 62, 293–302.
Kako, S., Isobe, A., Kubota, M., 2011b. High resolution ASCAT wind vector dataset gridded by applying an optimum interpolation method to the global ocean. J. Geophys. Res. 116, D23107. http://dx.doi.org/10.1029/2010JD015484.
Kako, S., Isobe, A., Magome, S., 2012. Low altitude remote-sensing method to monitor marine and beach litter of various colors using a balloon equipped with a digital camera. Mar. Pollut. Bull. 64, 1156–1162.
Kako, S., Isobe, A., Kataoka, T., Hinata, H., 2014. A decadal prediction of the quantity of plastic marine debris littered on beaches of the East Asian Marginal Seas. Mar. Pollut. Bull. 81, 174–184.
Kataoka, T., Hinata, H., Kako, S., 2012. A new technique for detecting colored macro plastic debris on beaches using webcam images and CIELUV. Mar. Pollut. Bull. 64, 1829–1836.
KNMI, 2010. MetOp-A ASCAT Level 2 25.0 km Ocean Surface Wind Vectors. Ver. Operational/Near-Real-Time. PO.DAAC, CA, USA Dataset accessed [2016-07-01].
Magome, S., Yamashita, T., Kohama, T., Kaneda, A., Hayami, Y., Takahashi, S., Takeoka, H., 2007. Jellyfish patch formation investigated by aerial photography and drifter experiment. J. Oceanogr. 63, 761–773.
Mato, Y., Isobe, T., Takada, H., Kanehiro, H., Ohtake, C., Kaminuma, T., 2001. Plastic resin pellets as a transport medium for toxic chemicals in the marine environment. Environ. Sci. Technol. 35, 318–324.
Murray, C.C., Bychkov, A., Therriaul, T., Hideaki, M., Wallace, N., 2015. The impact of Japanese tsunami marine debris on North America. PICES Press 23 (1), 28–30.
Nakashima, E., Isobe, A., Magome, S., Kako, S., Deki, N., 2011. Using aerial photography and in-situ measurements to estimate the quantity of macro-litter on beaches. Mar. Pollut. Bull. 62 (4), 762–776.
Nakashima, E., Isobe, A., Kako, S., Itai, T., Takahashi, S., 2012. Qualification of toxic metals derived from macroplastic litter on Ookushi beach, Japan. Environ. Sci. Technol. 46, 10099–10105.
Richardson, P.L., 1997. Drifting in the wind: leeway error in ship drift data. Deep-Sea Res. 44, 1878–1903.
Ryan, P.G., Moore, C.J., van Franeker, J.A., Moloney, C.L., 2009. Monitoring the abundance of plastic debris in the marine environment. Soc. B 364, 1992–2012. http://dx.doi.org/10.1098/rstb.2008.2007.
Veenstra, T.S., Churnside, J.H., 2012. Airborne sensors for detecting large marine debris at sea. Mar. Pollut. Bull. 65, 63–68.
Verspeek, J.A., Stoffelen, A., Portabella, M., Bonekamp, H., Anderson, C., Figa, J., 2009. Validation and calibration of ASCAT using CMOD5.n. IEEE Trans. Geosci. Remote Sens. 48 (1), 386–395 doi:10.1109/TGRS.2009.2027896.